nature plants

LETTERS

https://doi.org/10.1038/s41477-022-01238-3

Check for updates

Massive crossover suppression by CRISPR–Cas-mediated plant chromosome engineering

Michelle Rönspies[1], Carla Schmidt[1,2,3], Patrick Schindele[1], Michal Lieberman-Lazarovich[4], Andreas Houben[5] and Holger Puchta[1]✉

Recent studies have demonstrated that not only genes but also entire chromosomes can be engineered using clustered regularly interspaced short palindromic repeats (CRISPR)–CRISPER-associated protein 9 (Cas9)[1–5]. A major objective of applying chromosome restructuring in plant breeding is the manipulation of genetic exchange[6]. Here we show that meiotic recombination can be suppressed in nearly the entire chromosome using chromosome restructuring. We were able to induce a heritable inversion of a >17 Mb-long chromosome fragment that contained the centromere and covered most of chromosome 2 of the *Arabidopsis* ecotype Col-0. Only the 2 and 0.5 Mb-long telomeric ends remained in their original orientation. In single-nucleotide polymorphism marker analysis of the offspring of crosses with the ecotype Ler-1, we detected a massive reduction of crossovers within the inverted chromosome region, coupled with a shift of crossovers to the telomeric ends. The few genetic exchanges detected within the inversion all originated from double crossovers. This not only indicates that heritable genetic exchange can occur by interstitial chromosome pairing, but also that it is restricted to the production of viable progeny.

Clustered regularly interspaced short palindromic repeats (CRISPR)–CRISPER-associated protein (Cas)-based gene editing has revolutionized plant biology and breeding[7]. More and more tools are being developed to fine-tune both single and multiple gene modifications[8–10]. Being able to change the order of genes on a chromosome also adds a new level of trait control: the breakage of genetic linkages[11]. To combine attractive traits in a single cultivar, breeders rely on crossovers (CO) between parental homologous chromosomes by meiotic recombination[12]. It is well known that chromosomal rearrangements, such as inversions, modulate the recombination landscape along a chromosome by suppressing CO in the rearranged area[13–18]. For example, in *Drosophila*, so-called balancer chromosomes, which are characterized by multiple inversions and other rearrangements, are widely used, leading to the suppression of meiotic recombination in inversion heterozygotes[18]. Pan-genome studies have found that natural chromosomal rearrangements are prevalent in many crop species and have played an important role in domestication[4,19–24]. Despite their seemingly deleterious effects, inversions can also result in positive effects, such as the protection of favourable allelic combinations by preventing recombination[25]. Therefore, the targeted induction of chromosomal rearrangements by CRISPR–Cas has the potential to change meiotic recombination patterns. By reverting a 1.1 Mb-sized naturally derived inversion on chromosome 4 in the *Arabidopsis thaliana* ecotype Col-0, we could show that CO can be induced in a previously recombination-cold region[1].

In this study, we aimed to investigate whether we could exclude a substantial part of the *Arabidopsis* genome from genetic exchange by CRISPR–Cas-mediated chromosome engineering. To exclude as much genetic information as possible from meiotic recombination, we decided to invert nearly an entire chromosome and investigated the effect of the inversion on CO frequency and distribution. To achieve this goal, we used a well-established protocol for obtaining rare chromosome restructuring events in *Arabidopsis*[26]. By combining the *Staphylococcus aureus* orthologue of Cas9[27] with an egg cell-specific promoter, two double strand breaks (DSBs) were induced near the telomeric ends of chromosome 2 to invert the interjacent fragment with a size of 17.1 Mb. This left only a 2-Mb- and a 0.5-Mb-long telomeric end in their original orientation (Fig. 1a). The two selected guide sequences had both been previously used for the successful induction of inversions and translocations[28,29]. The selection and detection of the inversion were performed as previously described[1]. Out of the 40 screened T2 pools, one T2 pool was identified as positive for the inversion. Subsequently, the 40 descendants of the positive line were screened individually and one plant of the respective line was found to carry the inversion. The inversion junctions were amplified by PCR and sequenced to analyse the molecular nature of the junctions (Fig. 1b). The sequencing data revealed that the DNA ends were ligated precisely without any sequence loss or gain. To determine the genotype, the plant was also screened for the wildtype (WT) junctions and was found to carry the inversion hemizygously. The plant was grown until seed set and propagated. For subsequent experiments, T3 seeds were harvested and grown for 2 weeks on germination medium without selection and their genotype was determined by PCR screenings for the WT and inversion junctions. The phenotype of homozygous, hemizygous and WT plants did not differ from each other (Extended Data Fig. 1). The plants were also tested for segregation on the basis of Mendel's laws of segregation by using a chi-squared test with the critical value χ^2 (1; 0.95). Mendelian segregation was confirmed (Supplementary Table 1).

At the cytological level, chromosome inversion was confirmed in the hemizygous and homozygous mutant by fluorescence in situ hybridization (FISH). To obtain purely hemizygous seeds for the analysis, the homozygous inversion line was back-crossed with Col-0. Metaphase I meiocytes of the resulting F1 plants were prepared and BAC clones (Supplementary Table 2), which spanned

[1]Botanical Institute, Karlsruhe Institute of Technology, Karlsruhe, Germany. [2]Division of Cancer Research, Department of Thoracic Surgery, Medical Center - University of Freiburg, Faculty of Medicine, University of Freiburg, Freiburg, Germany. [3]German Cancer Consortium (DKTK) and German Cancer Research Center (DKFZ), Heidelberg, Germany. [4]Institute of Plant Sciences, Department of Vegetable and Field Crops, Agricultural Research Organization (ARO), Volcani Center, Rishon LeZion, Israel. [5]Leibniz Institute of Plant Genetics and Crop Plant Research (IPK), Seeland, Germany. ✉e-mail: holger.puchta@kit.edu

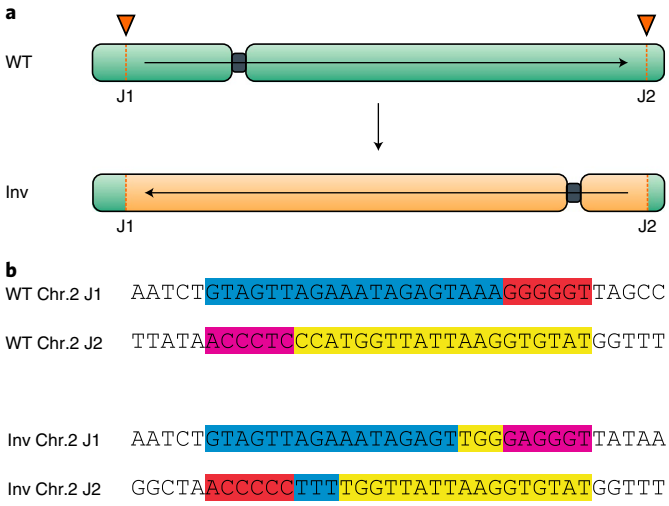

Fig. 1 | Schematic overview of the CRISPR–Cas9-induced chromosome inversion, WT and inversion junctions, fertility analysis and FISH analysis. a, Schematic overview of the induced chromosome inversion. Orange triangles and dashed lines indicate the location of the CRISPR–Cas9-induced DSB. **b**, DNA sequence of the two WT- and inversion-specific junctions. The 5′ guide sequence is highlighted in blue and the corresponding protospacer adjacent motif (PAM) sequence in red. The 3′ guide sequence is highlighted in yellow and the corresponding PAM sequence in pink. The first two lines show the original WT conformation. The last two lines show the junctions after induction of the inversion in their new conformation.

the two CRISPR–Cas9 cleavage sites, were chosen for red and green fluorescent labelling. In case of an inversion, both probes should be detected near each other. In WT, they should be located apart. Indeed, two separate signals were detected in WT (Fig. 2a). In the hemizygous sample, the WT signal pattern, as well as the inversion signal pattern were detected (Fig. 2a). Both newly formed junctions can be identified by adjacent red and green fluorescence signals. The FISH analysis of the hemizygous sample also shows that the WT chromosome and the chromosome carrying the inversion are indeed able to pair during meiosis. The pairing occurs outside of the inverted region at the telomeric end of chromosome 2 that carries a red label (Fig. 2a). Additionally, the inversion was confirmed in the homozygous mutant. In the homozygous sample, only the adjacent red and green fluorescence signals of the newly formed junctions were detected (Fig. 2a).

To assess the effect of the chromosomal rearrangement on fertility, a fertility assay was performed on homozygous, hemizygous and WT plants by counting the seed number of 10 siliques from 12 plants per genotype. We found that the seed number per silique was decreased by 1/3 in the hemizygous plants compared with homozygous and WT plants (Fig. 2b). Additionally, we observed empty spaces in place of seeds in several siliques of the hemizygous plants (Extended Data Fig. 2). The total seed number did not differ significantly between homozygous and WT plants.

Next, we investigated the effect of inverting approximately nine-tenths of the chromosome on the recombination frequency on chromosome 2 and, for purposes of control and comparison, on chromosome 3. The homozygous inversion line was crossed with Ler-1. F1 seeds were subsequently harvested. Then, they were propagated to obtain F2 seeds. The recombination frequency was determined by analysing 400 plants that were grown from F2 seeds. As a control, 400 plants of the progeny of crosses between WT Col-0 and Ler-1 were analysed. Using a *Taq*Man single-nucleotide polymorphism (SNP) genotyping assay, we selected 23 SNP markers on chromosome 2 and 9 SNP markers on chromosome 3 to detect marker changes between Col-0 and Ler-1 alleles (Supplementary Table 3). On chromosome 2, 8 SNP markers were selected within the inverted area. Outside of the inversion borders, 10 SNP markers were selected at the 5′ telomeric end and 5 markers at the 3′ telomeric end. The distance between the markers outside of the inversion was shorter to achieve a higher resolution of CO events at the telomere ends. The analysed plants were diploid; therefore, the marker analysis sums up the genetic state of two individual chromosomes that both underwent two meioses independently. Thus, we first analysed the presence or absence of marker changes in each sample.

In the offspring of the 'Inversion x Ler-1' (Inv x Ler-1) line, we detected a massive reduction of marker changes within the inverted area compared with the Col-0 x Ler-1 control. We detected 32 marker changes within the inverted region, compared with 386 in the Col-0 x Ler-1 control line in the same area. This corresponds to a roughly 92% reduction of recombination events in the inverted area of the Inv x Ler-1 line (Fig. 3a,b). Comparing the total number of marker changes detected outside of the inversion area in the Inv x Ler-1 line and the control, we found that the total number of marker changes was increased about 1.5-fold at the 5′ telomeric end and 2-fold at the 3′ telomeric end in the inversion line compared with the control line (Fig. 3a,b), pointing towards a shift of COs to the telomere ends as a consequence of the inversion. In total, we detected marker changes in 206 out of 400 samples on chromosome 2. As COs only need to occur in one of the two sister chromatids of a bivalent chromosome to ensure correct segregation, one would expect that about a quarter of the diploid progeny plants would show a lack of CO. We assume that the difference between the expected and detected number of non-recombinations is, at least in part, due to cases in which the CO required for chromosome segregation occurred at one of the subtelomeric ends outside of our tested marker intervals: about 68 kb on the 5′ telomeric end and about 21 kb on the 3′ telomeric end were not covered by our marker intervals. By comparison, in the offspring of the Col-0 x Ler-1 control, we detected marker changes in 331 out of 400 samples. No recombination was detected in 69 samples, which was in line with our expectations. In contrast to chromosome 2, no notable difference in CO distribution between the two crosses was detected on chromosome 3 in the same plants (Extended Data Fig. 3).

Subsequently, by analysing the marker change patterns in more detail (Fig. 3c–f and Extended Data Figs. 4–7), we deduced the genetic state of the individual chromosomes from the diploid genomes. In the Inv x Ler-1 line, of the 206 samples in which marker changes were detected, 142 samples had marker changes originating from a single CO on one chromosome (Fig. 3c,d). All of these single COs were located outside of the inversion in the unchanged subtelomeric ends: 128 samples had single COs detected at the 5′ telomeric end (Fig. 3c) and 14 samples at the 3′ telomeric end (Fig. 3d). Six samples showed a single CO at both telomeric ends (Fig. 3e). Forty-two samples showed marker changes originating from CO events that could not be clearly assigned to either of the two chromosomes (Extended Data Fig. 4a,b). Within the inversion, no single COs were detected. Among the 16 samples with detected marker changes within the inverted area, 9 samples showed marker changes originating from a double CO in one of the chromosomes (Fig. 3f). In 7 samples, we detected a double CO within the inversion, combined with a single CO at one telomeric end outside of the inversion (Extended Data Fig. 4c).

Out of the 331 samples with detected marker changes in the Col-0 x Ler-1 control, 204 samples had marker changes originating from single CO events (Extended Data Fig. 5). In 127 samples, we detected CO events originating either from a double CO in combination with a single CO, or from a combination of single COs stemming from two independent meioses (Extended Data Figs. 6 and 7).

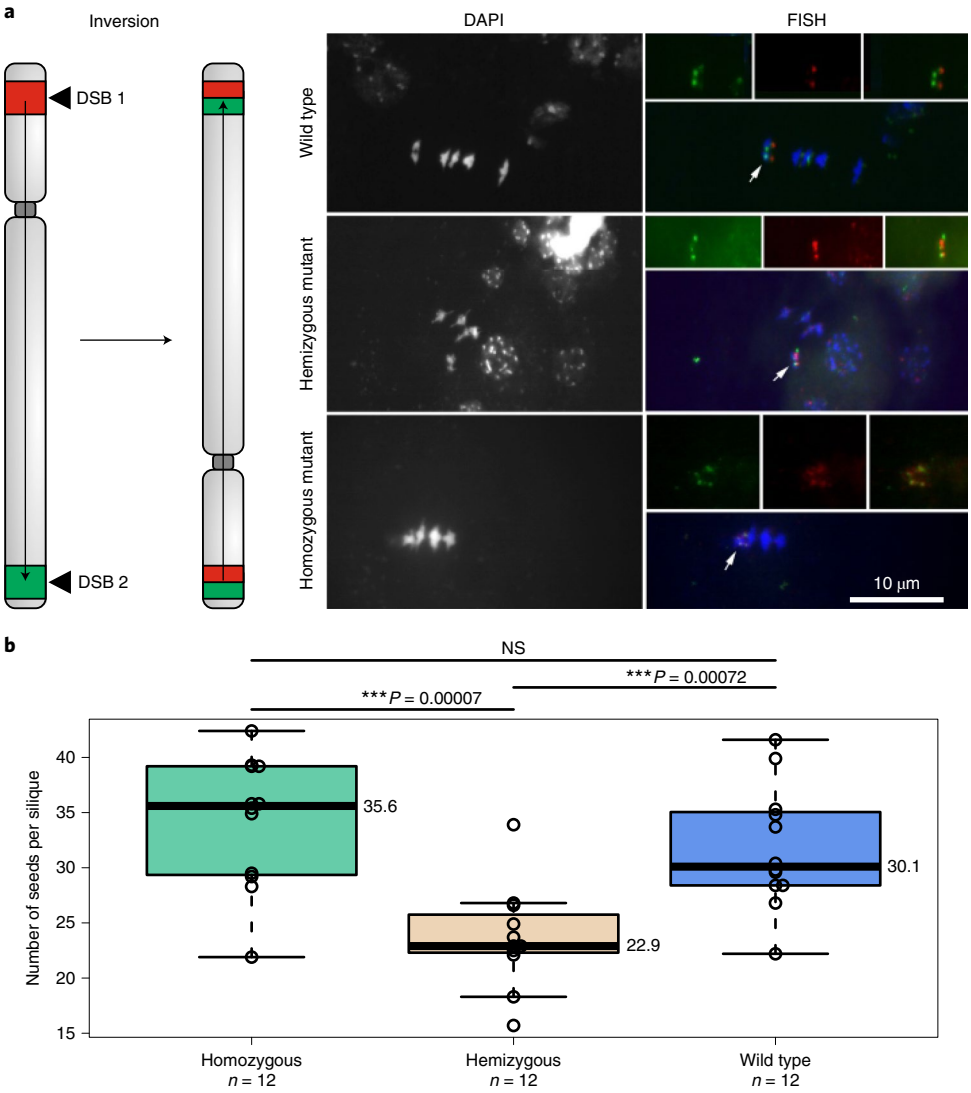

Fig. 2 | Fertility and FISH analyses. a, Overview of the FISH analysis of the hemizygous and homozygous inversion line. Left: schematic overview of the chromosome regions detected with fluorescently labelled BAC clones spanning the 5′ (red) and 3′ (green) cleavage sites. Black triangles indicate the location of the DSB. Induction of inversion leads to the presence of both fluorescence signals at both ends of the chromosome. Right: FISH results of the analysed metaphase I meiocytes of WT (top), hemizygous mutant (centre) and homozygous mutant (bottom). Left panel: DAPI. Right panel, from left to right (top row): FITC, Txred, FITC + Txred; bottom row: FITC + Txred + DAPI. White arrows indicate meiocytes in which the location of both fluorescently labelled BAC clones is visible. Two separate signals were detected in WT. In the hemizygous sample, the WT signal pattern, as well as the inversion signal pattern were detected. Both newly formed junctions can be identified by adjacent red and green fluorescence signals. In the homozygous sample, only the adjacent red and green fluorescence signals of the newly formed junctions were detected. **b**, Fertility analysis of homozygous, hemizygous and WT plants. Twelve homozygous, hemizygous and WT plants were randomly selected for fertility analysis ($n = 12$). Ten siliques per plant were randomly selected and the number of seeds per silique counted. The seed number of the hemizygous plants was significantly reduced, approximately by 1/3, compared with WT and homozygous plants. The seed number of homozygous and WT plants did not differ significantly. The boxplot shows the 12 independent biological replicates for each genotype. The average of the seed number of 10 siliques was calculated and is presented in the boxplots. The middle line represents the median, box edges represent the first and third quartiles, and whiskers extend to the minimum and maximum, respectively. Individual data points are represented as open circles. *P* values were calculated using a two-tailed *t*-test (***$P < 0.001$; NS, not significant).

As our marker analysis sums up the genetic state of two individual chromosomes that both underwent two meioses independently, it was not possible to clearly distinguish between double CO or multiple single CO events in the control line.

CO suppression in one area can lead to the enhancement of meiotic recombination on other chromosomes, which is referred to as interchromosomal effect and has been observed in various organisms[30]. In our experiments, we did not detect an increase of CO events on chromosome 3 in the Inv x Ler-1 line compared with the control. However, we did detect 1.5- and 2-fold increases in the number of marker changes on chromosome 2 outside of the inversion borders compared with the control. Therefore, the lack of COs within the inversion might have been compensated by an increased number of COs in the telomeric regions of chromosome 2 and the obligate CO required for proper segregation of the chromatids might have been shifted to both telomeric ends of the chromosome. The observed increase in recombination could also be due to the elimination of non-viable gametes with a single CO in the inversion, which would subsequently lead to the detection of an increased number of chromatids with CO outside of the

a

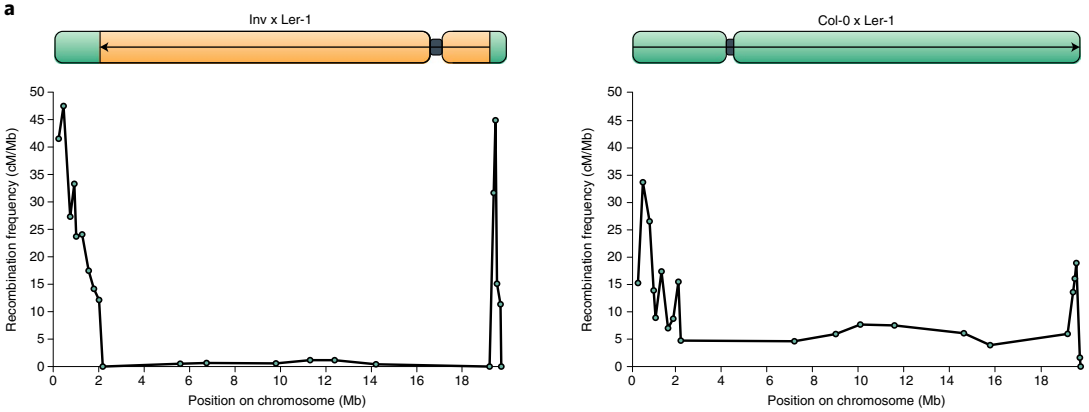

b

	5' telomeric end									Border	Inversion							Border	3' telomeric end				
	I1	I2	I3	I4	I5	I6	I7	I8	I9	I10	I11	I12	I13	I14	I15	I16	I17	I18	I19	I20	I21	I22
Inv x Ler-1	30	41	32	24	8	25	20	13	11	0	7	3	7	7	5	3	0	23	14	4	7	0
Col-0 x Ler-1	11	29	31	10	3	18	8	8	14	2	92	43	33	45	74	18	81	13	5	5	1	0
$Sum_{Inv\ x\ Ler-1}$						204								32						48		
$Sum_{Col-0\ x\ Ler-1}$						134								386						24		

c

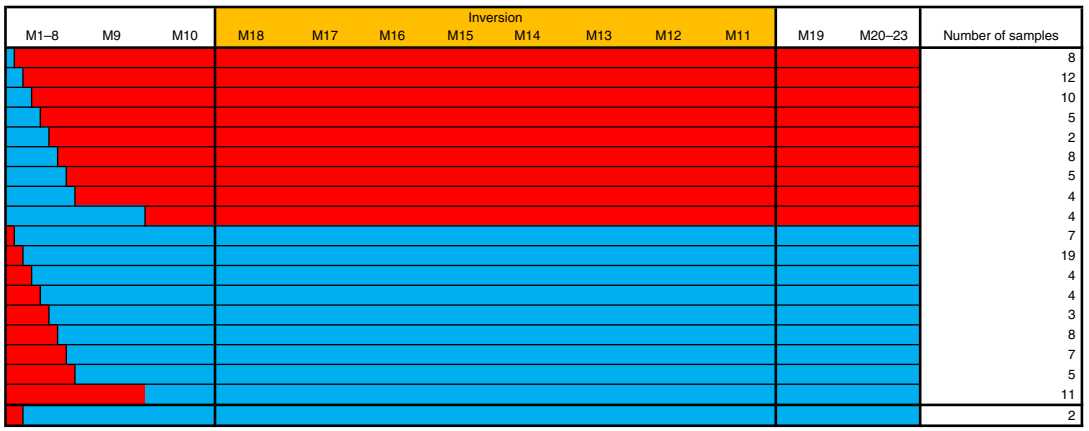

d

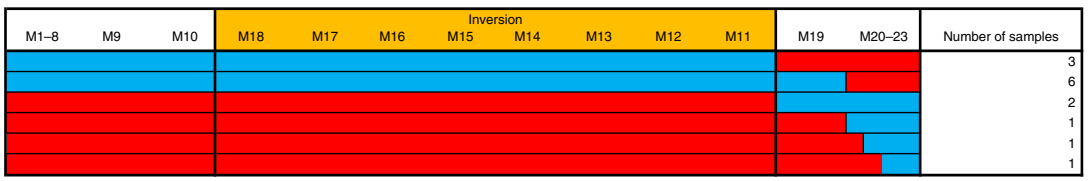

e

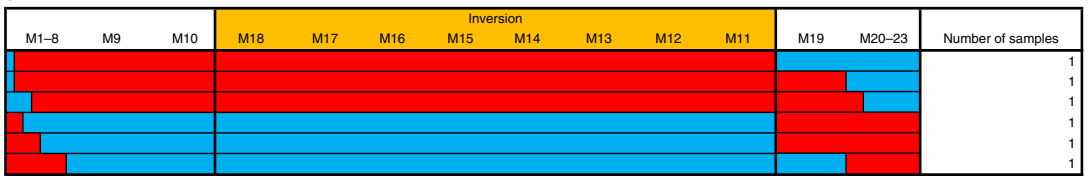

f

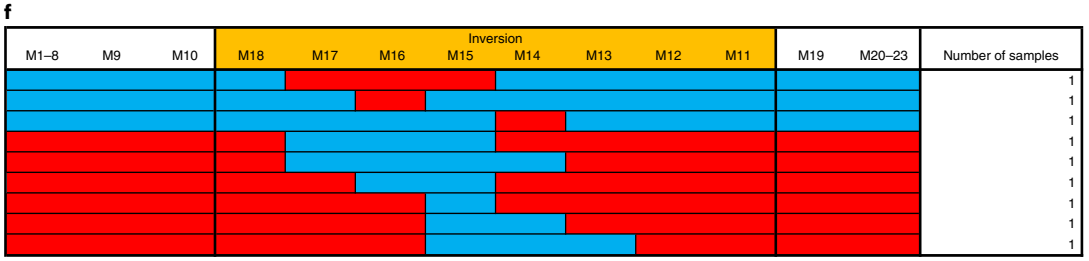

Fig. 3 | Recombination frequency on chromosome 2 and unambiguously assignable CO events in the inversion line. a, The recombination frequency on chromosome 2 was determined by SNP-based genotyping of 400 plants of the offspring of the Inv x Ler-1 line and the Col-0 x Ler-1 control. The recombination frequency is presented in cM/Mb. **b**, Overwiew of the total number of marker changes per marker interval (I1–22; Supplementary Table 3) outside and inside of the inverted area in the Inv x Ler-1 and Col-0 x Ler-1 lines. We detected a massive reduction of COs within the inversion borders, and 1.5- and 2-fold increases in marker changes at the 5′ and 3′ telomeric ends, respectively, compared with the control. Panel colour: grey background, intervals that lie outside the inverted area; light grey background, intervals covering the inversion sites; no background colour, intervals that lie inside the inverted area. **c**, Overview of marker changes that originated from a single CO on the 5′ telomeric end on one chromosome (126; rows 1–18) or from an identical single CO on both chromosomes (2; row 19). The Col-0 allele is represented by blue bars and the Ler-1 allele by red bars (same colour coding in **d**–**f**). **d**, Overview of marker changes that originated from a single CO on the 3′ telomeric end on one chromosome (14). **e**, Overview of marker changes that originated from a single CO on both telomeric ends of one chromosome (6). **f**, Overview of marker changes detected inside the inverted area, which can be clearly assigned to one of the two chromosomes. In 9 samples, marker changes inside the inversion that all originated from a double CO on one chromosome were detected. In another 7 samples, marker changes inside the inversion that originated from a combination of a double CO on one chromosome and a single CO on one or both chromosomes were detected. These samples are listed in Extended Data Fig. 4c.

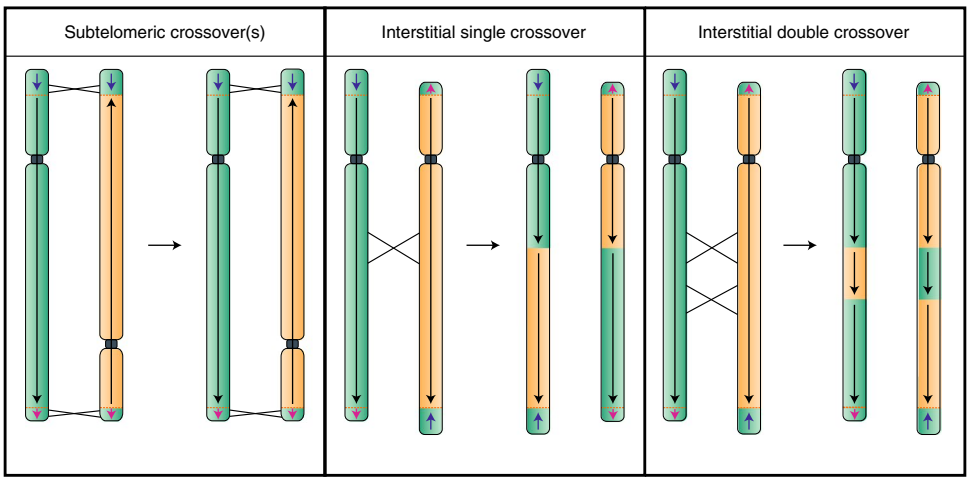

Fig. 4 | Consequences of the occurrence of subtelomeric, single or double COs in a large chromosome inversion. Left: pairing of the homologous regions of the unchanged distal chromosome regions, followed by single or double CO in the subtelomeric regions, results in viable gametes. Middle: pairing of the large homologous region within the inversion borders, followed by a single CO within the inverted area, leads to the loss of one telomeric end in both chromosomes, resulting in non-viable gametes. Right: pairing of the large homologous region within the inversion borders, followed by a double CO within the inverted area, leads to viable gametes as no genetic information is lost.

inversion. In line with this observation, we were able to detect pairing of a WT chromosome and a chromosome carrying the inversion at the telomeric end of the smaller arm of chromosome 2 in our cytological analysis.

Applying our CRISPR–Cas-based strategy for inverting chromosomal regions[29], we were able to invert almost nine-tenths of chromosome 2 in *Arabidopsis*, which led to a near-complete exclusion of more than one-tenth of the *Arabidopsis* genome from genetic exchange. Indeed, within the inversion borders, the number of marker changes was drastically reduced (by 92% compared with the control), although recombination was not completely abolished. In 4% of the samples, double COs were detected within the inverted region, indicating that in rare cases, meiotic pairing and recombination can occur within the inverted region and can lead to viable gametes. However, as known from *Drosophila*, a single CO between a chromosome carrying a pericentric inversion and its WT homologue leads to the formation of chromosomes carrying duplications or deletions, which ultimately causes embryonic lethality[18]. In the case of the induced 17.1 Mb inversion, a single CO within the inverted area led to the formation of two *Arabidopsis* chromosomes carrying two identical telomeric ends as opposed to differing 5′ and 3′ telomeric ends (Fig. 4). This results in a massive loss of genetic information and, therefore, non-viable progeny. In contrast, as shown in Fig. 4, only COs in the telomeric ends or double COs within the inversion can lead to the formation of viable gametes. In its hemizygous state, the inversion led to a notable reduction (by about one third) of viable seeds, whereas the homozygous mutant was fully fertile. The simplest explanation is that in about every third meiosis, the presence of the inversion hindered the formation of viable gametes due to the occurrence of single CO events within the inversion. However, the majority of seeds were still viable, making the exclusion of large parts of the genome from meiotic recombination by chromosome engineering a nonetheless useful tool for breeders to maintain favourable genetic linkages. This is also supported by the fact that natural inversions do not always lead to measurable fertility defects[31,32].

Our study shows that it is possible to suppress recombination at the chromosomal level in a multicellular eukaryote by CRISPR–Cas-mediated chromosome engineering. We were able to develop a new instrument for the ever-growing toolbox of genome engineering, allowing the suppression of recombination anywhere in the genome in a predesigned fashion. This approach should be widely feasible among eukaryotes. Moreover, we showed that it is possible to almost completely abolish recombination in nearly an entire chromosome representing a substantial part of the *Arabidopsis* genome.

Accordingly, our results have important consequences for plant breeding, as they demonstrate that chromosome engineering can be a valuable tool for breeders in excluding favourable allelic combinations of any size from recombination, thereby stabilizing genetic linkages.

Methods

Cloning of T-DNA constructs. Cloning of the transfer DNA (T-DNA) constructs was based on the Gateway-compatible plasmids pEn-Sa-Chimera and pDe-Sa-Cas9 with *S. aureus* Cas9 under the control of an egg cell-specific promotor (pDe-Sa-Cas9 EC)[1,27]. The spacer sequences (Supplementary Table 4) were cloned as annealed oligonucleotides into individual pEn-Sa-Chimera vectors via BbsI restriction digest. Via MluI restriction digest, the first guide RNA (gRNA) cassette was integrated into pDe-Sa-Cas9 EC. The second gRNA cassette was transferred via a Gateway LR reaction.

Plant cultivation and transformation. *A. thaliana* seeds were stratified overnight at 4 °C and transferred to soil consisting of a 1:1 mixture of Floraton 3 (Floragard) and vermiculite (2–3 mm, Deutsche Vermiculite Dämmstoff). For propagation, the plants were cultivated in the greenhouse under 16 h light/8 h dark conditions at 22 °C for 6–7 weeks until seed set. For transformation, 4–5-week-old Col-0 plants were transformed with the CRISPR–Cas expression construct via *Agrobacterium*-mediated floral dip transformation. The transformed plants were cultivated for 4–5 weeks until seed set. For sterile plant culture, seeds were surface-sterilized with 4% sodium hypochlorite and stratified overnight at 4 °C. For transgenic plant selection, the stratified seeds were sowed on germination medium (4.9 g l^{-1} Murashige and Skoog medium, 10 g l^{-1} saccharose, pH 5.7 and 7.6 g l^{-1} plant agar) with phosphinotricin and cefotaxime. T1 plants were propagated in the greenhouse and the seeds harvested. T2 seeds were stratified and sowed on the germination medium without further additives. The plates were placed in a growth chamber at 22 °C under 16 h light/8 h dark conditions for 2 weeks.

DNA extraction. For individual plant screenings, one leaf per plant was cut off and separately placed into a 1.5 ml reaction tube. For bulk screenings, one leaf each from 40 plants was cut off and leaves combined in the same 1.5 ml reaction tube. The plant material was ground with a pestle and 500 µl extraction buffer (200 mM Tris-HCl (pH 9.0), 400 mM LiCl, 25 mM EDTA, 1% SDS, pH 9.0) was added to the tubes. The mixture was centrifuged for 5 min at 17,000 *g* at room temperature. The supernatant (400 µl) was transferred to a new 1.5 ml tube containing 400 µl 2-propanol. The sample was thoroughly inverted and the DNA was pelleted for 10 min at 19,500 *g* at room temperature. The supernatant was discarded and the pellet was dried either for 1.5 h at 37 °C or overnight at room temperature. Afterwards, the pellets were resuspended in 50 µl (individual DNA extraction) or 100 µl (bulk DNA extraction) TE buffer (10 mM Tris-HCl (pH 9.0), 1.0 mM EDTA, pH 8.0).

Establishment of the homozygous inversion line. T2 seeds were cultivated on germination medium for 2 weeks in a growth chamber. Subsequently, bulk DNA extractions were performed with 40 plants per T2 line. These T2 pools were screened for the presence of the inversion via PCR using junction-specific primers (Supplementary Table 4). Sequencing of the junctions was performed by Eurofins Genomics, and the software ApE (v2.0.55) was used for alignment and analysis of Sanger sequencing data. One T2 line tested positive for the inversion. The individual plants of this line were subjected to individual DNA extraction to identify the individual plants harbouring the rearrangement. The individual DNA samples were again screened by PCR. The identified positive plant was transferred to the greenhouse and grown for 6–7 weeks until seed set. In the T3 generation, the seeds were genotyped by PCR using primers specific for the WT and inversion junctions (Supplementary Table 4). The line was also tested for Mendelian segregation on the basis of the genotyping results using a chi-squared test with the critical value χ^2 (1; 0.95). Homozygous plants and, as a control, Col-0 plants were crossed with the Ler-1 ecotype for subsequent determination of CO frequencies. F1 seeds were propagated in the greenhouse and ripe F2 seeds were harvested after 6–7 weeks.

Phenotypic analysis and fertility assays. Homozygous, hemizygous and WT plants, as determined by PCR-based genotyping in the T3 generation, were grown in the greenhouse for 5–6 weeks under 16 h light/8 h dark conditions at 22 °C. After representative pictures were taken for phenotype analysis, 10 mature siliques of 12 plants per line were collected and incubated overnight in 70% EtOH to determine the effects of the inversion on fertility. The number of seeds per silique was counted and pictures of the siliques were taken using a binocular microscope. *P* values were calculated using a two-tailed *t*-test. Graphs were created using R Studio (Version 1.1.423) and CorelDRAW 2020 (Version 22.1.1.523).

Determination of CO frequency. CO frequency was determined by the detection of marker changes via SNP-based genotyping using cultivar-specific probes. For chromosome 2, 23 *Taq*Man probes and specific primers were designed. For chromosome 3, 9 *Taq*Man SNP genotyping assays were designed. All probes and primers are listed in Supplementary Tables 3 and 4. The analysis was performed using a Lightcycler 480 II (Roche) and the PerfeCTa qPCR ToughMix (Quantabio) according to the manufacturer's protocol but with a total reaction volume of 10 µl. The data were analysed with LightCycler 480 SW 1.5. Graphs were created using Microsoft Excel 2016 and CorelDRAW 2020 (Version 22.1.1.523).

FISH. FISH analysis was performed using differently labelled DNA probes specific for the inversion breakpoint regions of chromosome 2. Pools of contiguous BAC clones of chromosome 2 were used to paint the neighbouring regions of the CRISPR–Cas9 cleavage sites (Supplementary Table 2)[33]. An epifluorescence microscope (BX-61, Olympus) equipped with a UPlan(F) ×100/1.30 objective lens (Olympus) and a cooled black/white CCD camera (ORCA-R2, Hamamatsu), under the control of the microscope software CellSens Dimension (Olympus) was used to record the micrographs. The following fluorescence filters were used: FITC-2024B-000, Txred-4040C-000n and Sp. Aqua HC (Sembrock). Black and white pictures were pseudo-coloured with the software Photoshop 2020 (Adobe).

Reporting summary. Further information on research design is available in the Nature Research Reporting Summary linked to this article.

Data availability

The data supporting the findings are available within the article or in Supplementary Information. Source data for Figs. 2b, 3a,b and Extended Data Fig. 3 are provided with this paper.

Received: 13 January 2022; Accepted: 2 July 2022;
Published online: 15 September 2022

References

1. Schmidt, C. et al. Changing local recombination patterns in *Arabidopsis* by CRISPR/Cas mediated chromosome engineering. *Nat. Commun.* **11**, 4418 (2020).
2. Beying, N., Schmidt, C., Pacher, M., Houben, A. & Puchta, H. CRISPR–Cas9-mediated induction of heritable chromosomal translocations in *Arabidopsis*. *Nat. Plants* **6**, 638–645 (2020).
3. Lu, Y. et al. A donor-DNA-free CRISPR/Cas-based approach to gene knock-up in rice. *Nat. Plants* **7**, 1445–1452 (2021).
4. Schwartz, C. et al. CRISPR–Cas9-mediated 75.5-Mb inversion in maize. *Nat. Plants* **6**, 1427–1431 (2020).
5. Filler Hayut, S., Melamed Bessudo, C. & Levy, A. A. Targeted recombination between homologous chromosomes for precise breeding in tomato. *Nat. Commun.* **8**, 15605 (2017).
6. Rönspies, M., Dorn, A., Schindele, P. & Puchta, H. CRISPR–Cas-mediated chromosome engineering for crop improvement and synthetic biology. *Nat. Plants* **7**, 566–573 (2021).
7. Gao, C. Genome engineering for crop improvement and future agriculture. *Cell* **184**, 1621–1635 (2021).
8. Molla, K. A., Qi, Y., Karmakar, S. & Baig, M. J. Base editing landscape extends to perform transversion mutation. *Trends Genet.* **36**, 899–901 (2020).
9. Atkins, P. A. & Voytas, D. F. Overcoming bottlenecks in plant gene editing. *Curr. Opin. Plant Biol.* **54**, 79–84 (2020).
10. Schindele, A., Dorn, A. & Puchta, H. CRISPR/Cas brings plant biology and breeding into the fast lane. *Curr. Opin. Biotechnol.* **61**, 7–14 (2020).
11. Lee, K. & Wang, K. Level up to chromosome restructuring. *Nat. Plants* **6**, 600–601 (2020).
12. Blary, A. & Jenczewski, E. Manipulation of crossover frequency and distribution for plant breeding. *Theor. Appl. Genet.* **132**, 575–592 (2019).
13. Sturtevant, A. H. A case of rearrangement of genes in *Drosophila*. *Proc. Natl Acad. Sci. USA* **7**, 235–237 (1921).
14. Crown, K. N., Miller, D. E., Sekelsky, J. & Hawley, R. S. Local inversion heterozygosity alters recombination throughout the genome. *Curr. Biol.* **28**, 2984–2990 (2018).
15. Huang, K. & Rieseberg, L. H. Frequency, origins, and evolutionary role of chromosomal inversions in plants. *Front. Plant Sci.* **11**, 296 (2020).
16. Kirkpatrick, M. & Barton, N. Chromosome inversions, local adaptation and speciation. *Genetics* **173**, 419–434 (2006).
17. Coughlan, J. M. & Willis, J. H. Dissecting the role of a large chromosomal inversion in life history divergence throughout the *Mimulus guttatus* species complex. *Mol. Ecol.* **28**, 1343–1357 (2019).
18. Miller, D. E., Cook, K. R. & Hawley, R. S. The joy of balancers. *PLoS Genet.* **15**, e1008421 (2019).
19. Walkowiak, S. et al. Multiple wheat genomes reveal global variation in modern breeding. *Nature* **588**, 277–283 (2020).
20. Jayakodi, M. et al. The barley pan-genome reveals the hidden legacy of mutation breeding. *Nature* **588**, 284–289 (2020).
21. Crow, T. et al. Gene regulatory effects of a large chromosomal inversion in highland maize. *PLoS Genet.* **16**, e1009213 (2020).
22. Liu, Y. et al. Pan-genome of wild and cultivated soybeans. *Cell* **182**, 162–176 (2020).
23. Alonge, M. et al. Major impacts of widespread structural variation on gene expression and crop improvement in tomato. *Cell* **182**, 145–161 (2020).
24. Qin, P. et al. Pan-genome analysis of 33 genetically diverse rice accessions reveals hidden genomic variations. *Cell* **184**, 3542–3558 (2021).
25. Fransz, P. et al. Molecular, genetic and evolutionary analysis of a paracentric inversion in *Arabidopsis thaliana*. *Plant J.* **88**, 159–178 (2016).

26. Rönspies, M., Schindele, P., Wetzel, R. & Puchta, H. CRISPR–Cas9-mediated chromosome engineering in *Arabidopsis thaliana*. *Nat. Protoc.* **17**, 1332–1358 (2022).
27. Steinert, J., Schiml, S., Fauser, F. & Puchta, H. Highly efficient heritable plant genome engineering using Cas9 orthologues from *Streptococcus thermophilus* and *Staphylococcus aureus*. *Plant J.* **84**, 1295–1305 (2015).
28. Beying, N., Schmidt, C., Pacher, M., Houben, A. & Puchta, H. CRISPR–Cas9-mediated induction of heritable chromosomal translocations in *Arabidopsis*. *Nat. Plants* **6**, 638–645 (2020).
29. Schmidt, C., Pacher, M. & Puchta, H. Efficient induction of heritable inversions in plant genomes using the CRISPR/Cas system. *Plant J.* **98**, 577–589 (2019).
30. Termolino, P. et al. Recombination suppression in heterozygotes for a pericentric inversion induces the interchromosomal effect on crossovers in *Arabidopsis*. *Plant J.* **100**, 1163–1175 (2019).
31. Coyne, J. A., Aulard, S. & Berry, A. Lack of underdominance in a naturally occurring pericentric inversion in *Drosophila melanogaster* and its implications for chromosome evolution. *Genetics* **129**, 791–802 (1991).
32. Coyne, J. A., Meyers, W., Crittenden, A. P. & Sniegowski, P. The fertility effects of pericentric inversions in *Drosophila melanogaster*. *Genetics* **134**, 487–496 (1993).
33. Lysak, M. A., Fransz, P. F., Ali, H. B. & Schubert, I. Chromosome painting in *Arabidopsis thaliana*. *Plant J.* **28**, 689–697 (2001).

Acknowledgements

We thank J. Baumann, N. Schäfter and K. Kumke for their excellent technical assistance and D. Donahey for proofreading the manuscript. This research was funded by the European Research Council (Grant number ERC-2016-AdG_741306 CRISBREED) to H.P.

Author contributions

M.R., C.S. and H.P. designed and planned the experiments. M.R., C.S, M.L.-L. and A.H. carried out the experiments. M.R., C.S., P.S, A.H. and H.P. analysed data. M.R. and P.S. created the figures and M.R., P.S., A.H. and H.P. wrote the paper.

Competing interests

The authors declare no competing interests.

Additional information

Extended data is available for this paper at https://doi.org/10.1038/s41477-022-01238-3.

Supplementary information The online version contains supplementary material available at https://doi.org/10.1038/s41477-022-01238-3.

Correspondence and requests for materials should be addressed to Holger Puchta.

Peer review information *Nature Plants* thanks Ian Henderson and the other, anonymous, reviewer(s) for their contribution to the peer review of this work.

Reprints and permissions information is available at www.nature.com/reprints.

Publisher's note Springer Nature remains neutral with regard to jurisdictional claims in published maps and institutional affiliations.

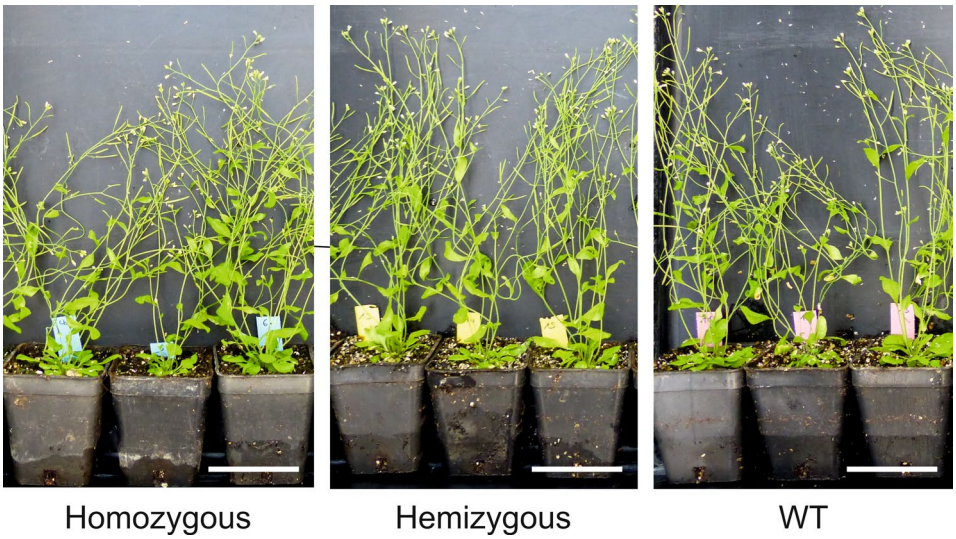

Extended Data Fig. 1 | Phenotype analysis of homozygous, hemizygous and WT plants. Representative pictures were taken from three homozygous, hemizygous and WT plants at 7.5 weeks-old. No phenotypic differences were observed. Scale bars represent 5 cm. Experiments were repeated two times independently with similar results.

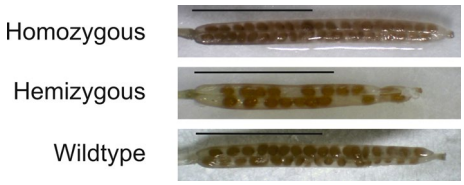

Extended Data Fig. 2 | Representative siliques from homozygous, hemizygous and WT plants. We observed empty spaces in place of seeds in several siliques of the hemizygous plants. Pictures were obtained while performing the fertility analysis of homozygous, hemizygous and WT plants with 12 plants per genotype which were randomly selected and 10 randomly selected siliques per plant (Fig. 2b). Scale bars represent 5 mm. Experiments were repeated two times independently with similar results.

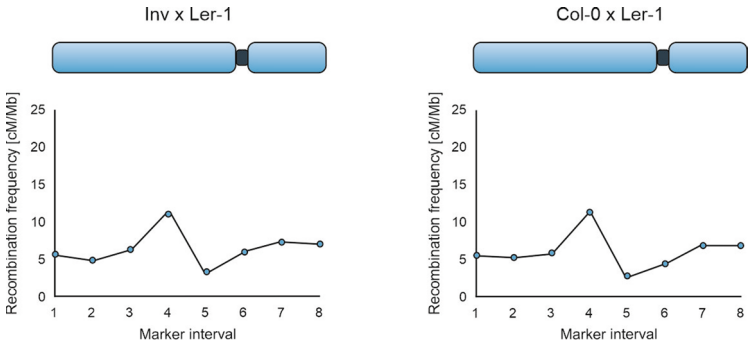

Extended Data Fig. 3 | Recombination frequency on chromosome 3. The recombination frequency on chromosome 3 was determined by SNP-based genotyping of 400 plants of the offspring of the *Inversion x Ler-1* line (Inv x Ler-1) and the control, Col-0 x Ler-1 for each marker interval (I1-8; Supplementary Table 3). The recombination frequency is presented in cM/Mb. No notable difference in CO distribution between the two crosses on chromosome 3 was detected. Source data are provided as Source Data file.

a

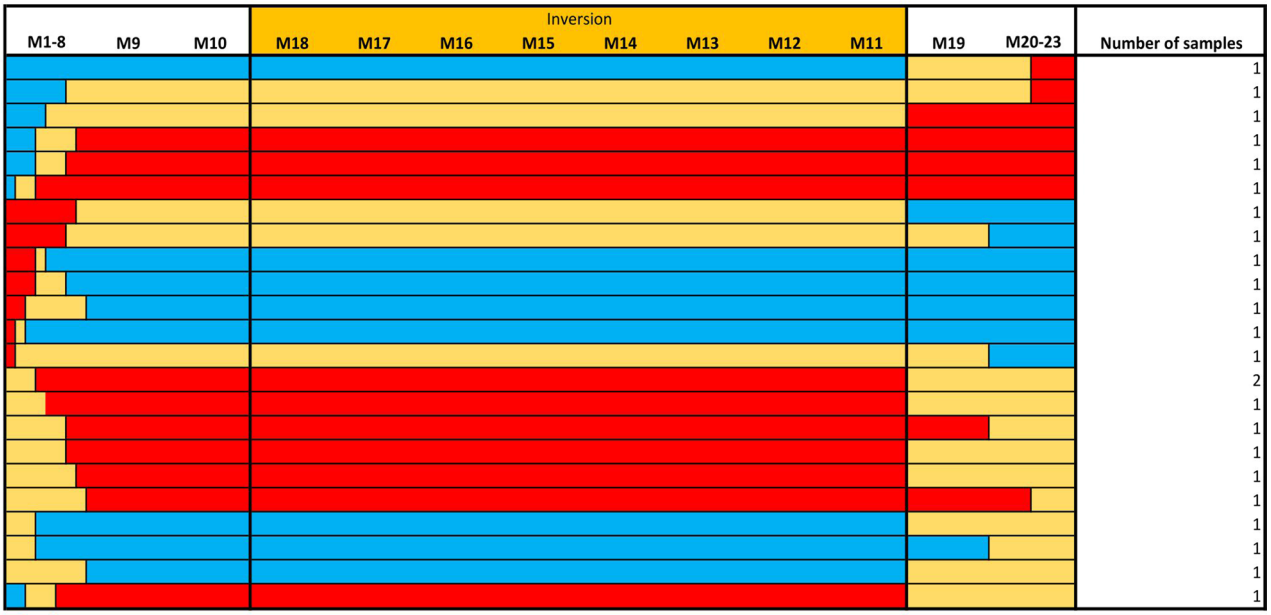

b

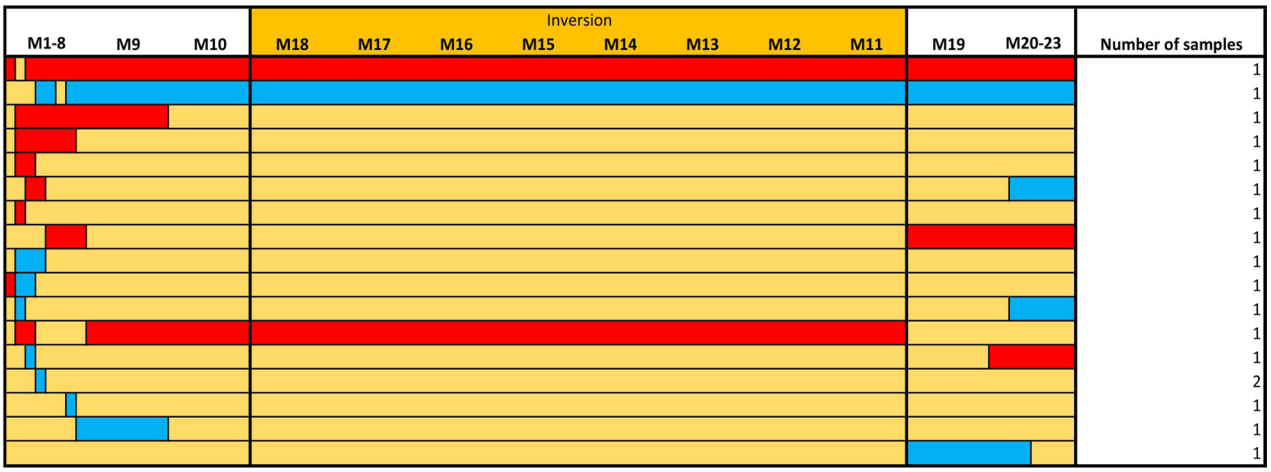

c

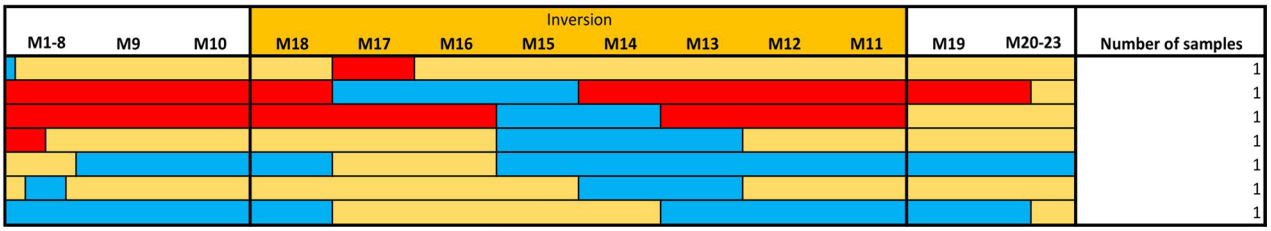

Extended Data Fig. 4 | Overview of the detected CO events in the *Inversion x Ler-1* line on chromosome 2 which cannot be clearly assigned to one of the two chromosomes. The Col-0 allele is represented by blue bars and the Ler-1 allele by red bars. The detection of both alleles is represented by yellow bars. **a**, Overview of marker changes which originated from differing single CO on both chromosomes (24). **b**, Overview of marker changes which originated either from differing single CO on one or both chromosomes or from double CO outside of the inversion or a combination of double CO outside of the inversion with differing single CO (18). **c**, In 7 samples, marker changes inside the inversion were detected which originated from a combination of a double CO on one chromosome and single CO on one or both chromosomes.

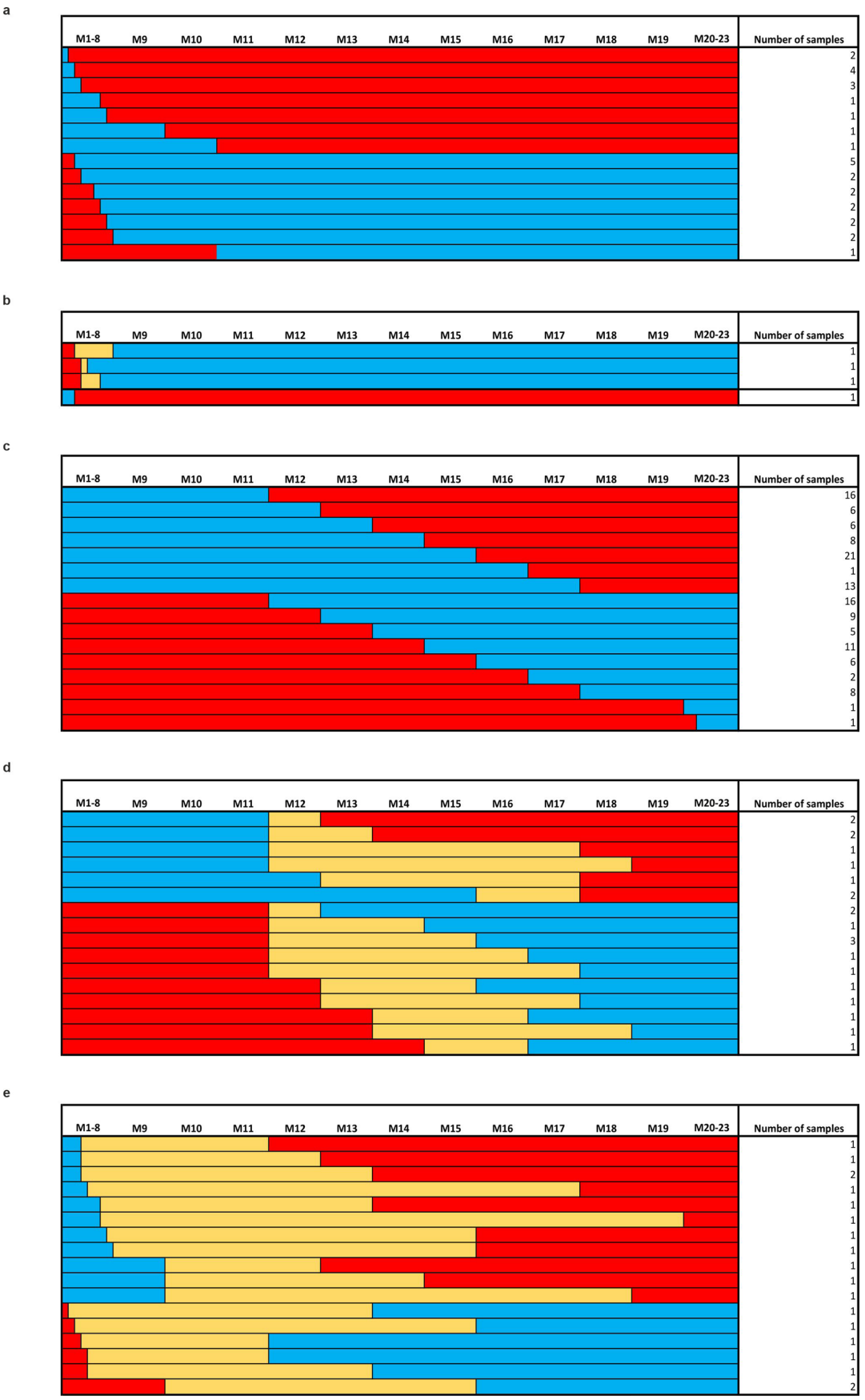

Extended Data Fig. 5 | See next page for caption.

Extended Data Fig. 5 | Overview of the detected single CO events in the Col-0 x Ler-1 line on chromosome 2. The Col-0 allele is represented by blue bars and the Ler-1 allele by red bars. The detection of both alleles is represented by yellow bars. **a**, Overview of marker changes which originated from single CO on the short arm on one chromosome (29). **b**, Overview of marker changes which originated from a differing single CO on the short arm on both chromosomes (3; rows 1–3) or two identical single CO on both chromosomes (1; row 4). **c**, Overview of marker changes which originated from single CO on the long arm on one chromosome (130). **d**, Overview of marker changes which originated from differing single CO on the long arm of both chromosomes (22). **e**, Overview of marker changes which originated from differing single CO, one on the long and one of the short arm of either chromosome (19).

a

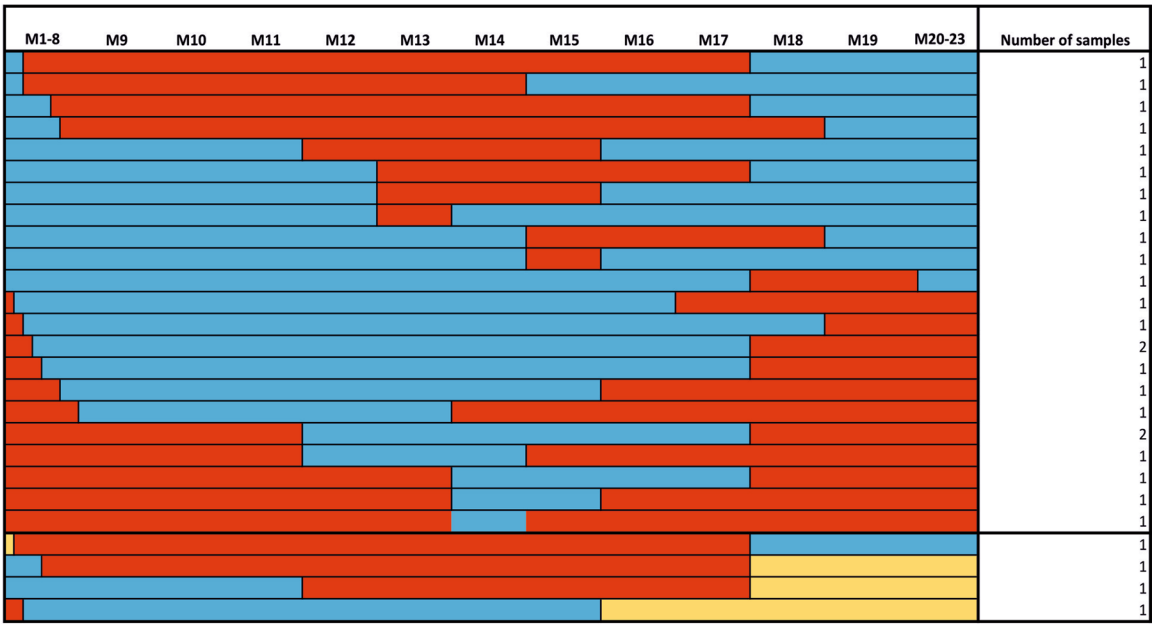

b

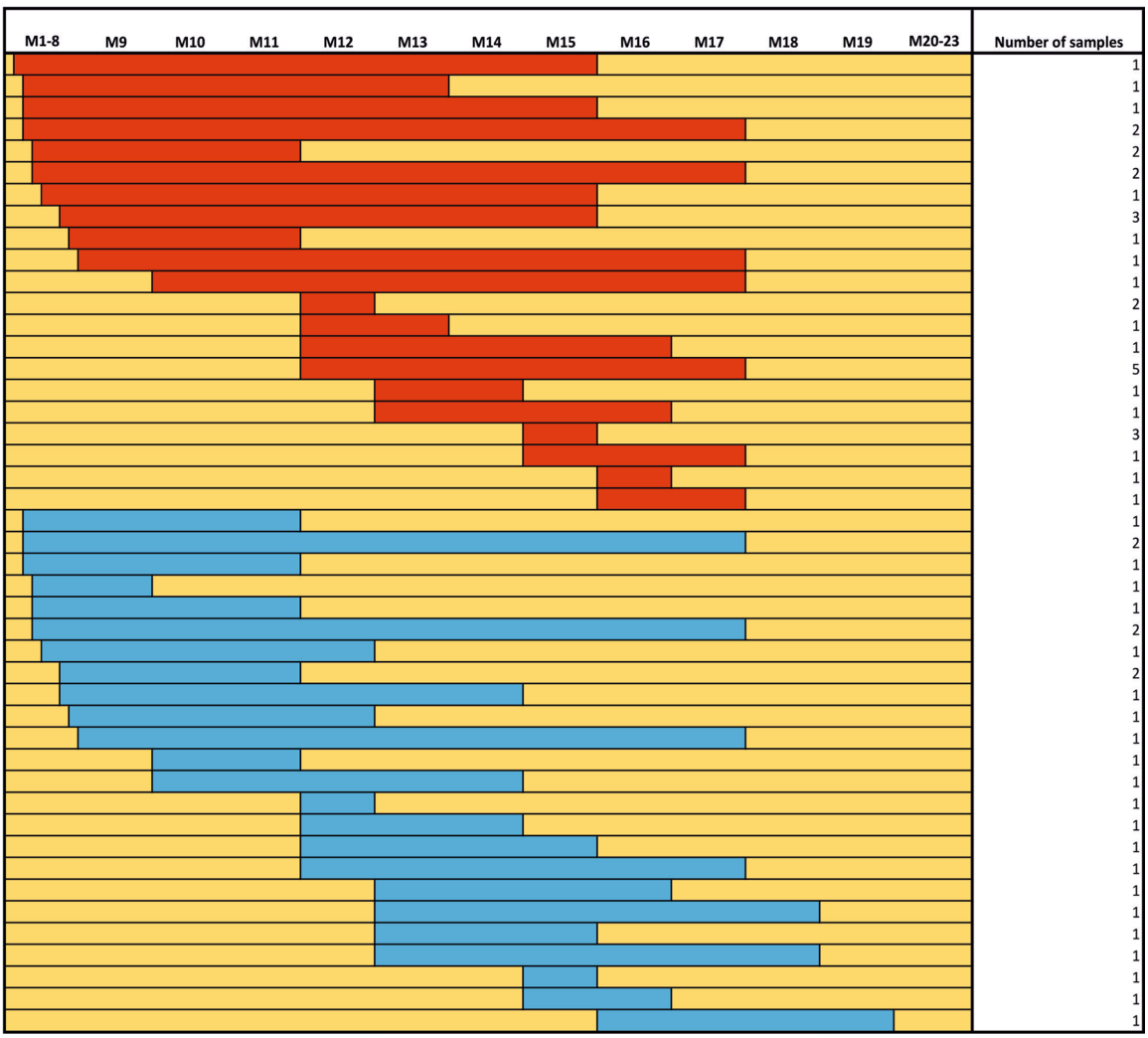

Extended Data Fig. 6 | See next page for caption.

Extended Data Fig. 6 | Overview of the detected double and/or single CO events in the Col-0 x Ler-1 line on chromosome 2. The Col-0 allele is represented by blue bars and the Ler-1 allele by red bars. The detection of both alleles is represented by yellow bars. **a**, Overview of marker changes which originated either from a double CO on one chromosome or from two single CO from two different meioses on one chromosome (24; rows 1–22) and from a combination of either a double CO on one chromosome and a single CO on the other chromosome or two single CO from different meioses on one chromosome and a single CO on the other chromosome (4; rows 23–26). **b**, Overview of marker changes which originated either from a double CO on one chromosome or from two single CO from two different meioses on one chromosome (60).

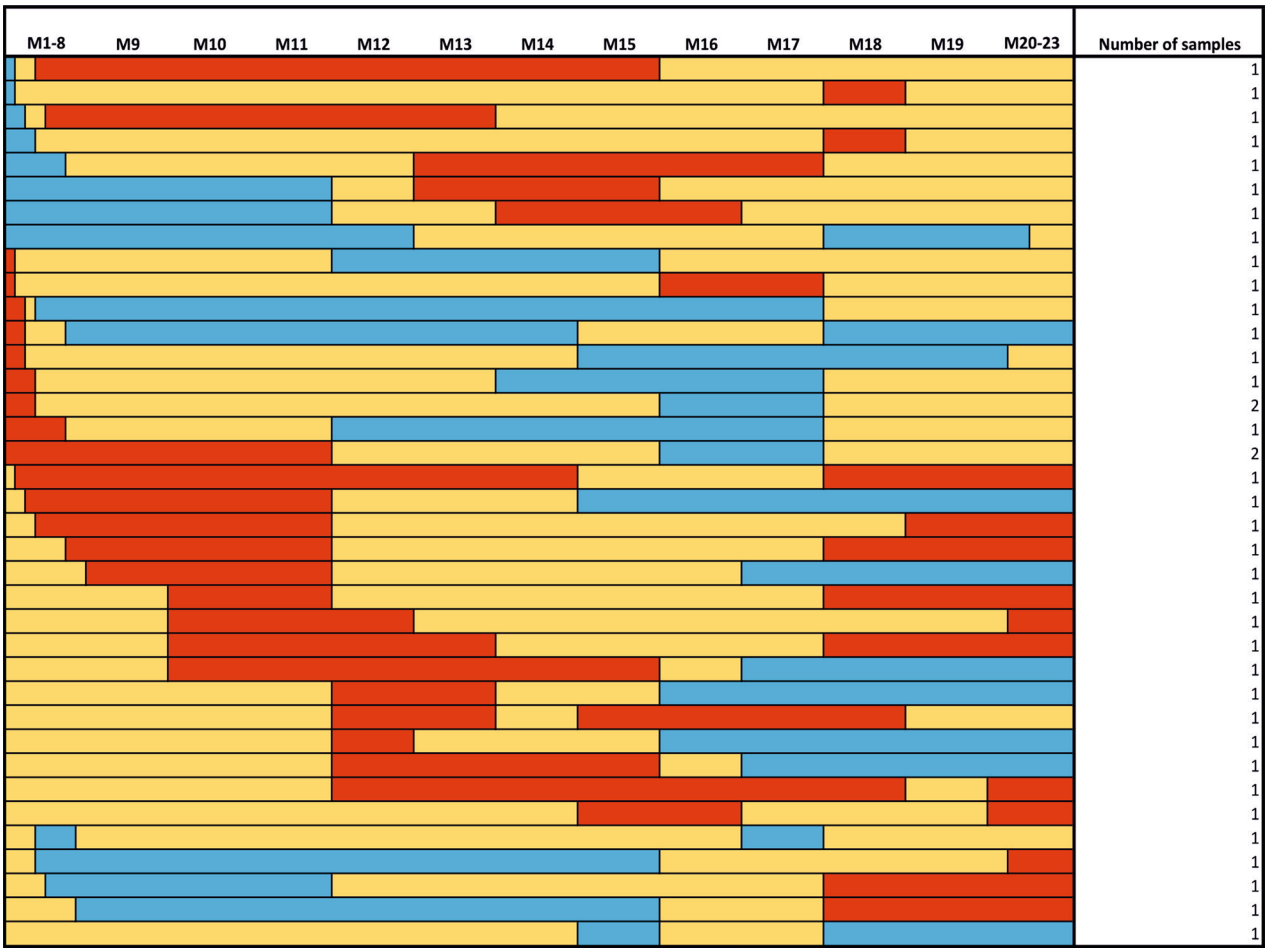

Extended Data Fig. 7 | Overview of the detected double and/or single CO events in the Col-0 x Ler-1 line on chromosome 2 which could not be unamigously assigned to either of the chromosomes. The Col-0 allele is represented by blue bars and the Ler-1 allele by red bars. The detection of both alleles is represented by yellow bars. Overview of marker changes which could not be unamigously assigned to either of the chromosomes and originated either from a combination of double CO and single CO on one or both chromosomes or differing single CO from two meioses (39).

nature portfolio

Corresponding author(s): Holger Puchta

Last updated by author(s): Jun 30, 2022

Reporting Summary

Nature Portfolio wishes to improve the reproducibility of the work that we publish. This form provides structure for consistency and transparency in reporting. For further information on Nature Portfolio policies, see our Editorial Policies and the Editorial Policy Checklist.

Statistics

For all statistical analyses, confirm that the following items are present in the figure legend, table legend, main text, or Methods section.

n/a	Confirmed
☐	☒ The exact sample size (*n*) for each experimental group/condition, given as a discrete number and unit of measurement
☐	☒ A statement on whether measurements were taken from distinct samples or whether the same sample was measured repeatedly
☐	☒ The statistical test(s) used AND whether they are one- or two-sided *Only common tests should be described solely by name; describe more complex techniques in the Methods section.*
☒	☐ A description of all covariates tested
☒	☐ A description of any assumptions or corrections, such as tests of normality and adjustment for multiple comparisons
☐	☒ A full description of the statistical parameters including central tendency (e.g. means) or other basic estimates (e.g. regression coefficient) AND variation (e.g. standard deviation) or associated estimates of uncertainty (e.g. confidence intervals)
☐	☒ For null hypothesis testing, the test statistic (e.g. *F*, *t*, *r*) with confidence intervals, effect sizes, degrees of freedom and *P* value noted *Give P values as exact values whenever suitable.*
☒	☐ For Bayesian analysis, information on the choice of priors and Markov chain Monte Carlo settings
☒	☐ For hierarchical and complex designs, identification of the appropriate level for tests and full reporting of outcomes
☒	☐ Estimates of effect sizes (e.g. Cohen's *d*, Pearson's *r*), indicating how they were calculated

Our web collection on statistics for biologists contains articles on many of the points above.

Software and code

Policy information about availability of computer code

Data collection	No custom code was used in data collection. Sequence information was obtained from TAIR (https://arabidopsis.org/) and Arabidopsis 1,001 Genome Browser (http://signal.salk.edu/atg1001/3.0/gebrowser.php). Sanger sequencing was performed by Eurofins Genomics. For gel documentation, the automated imaging system GEL iX IMager (Intas) was used. An epifluorescence microscope (BX-61, Olympus), equipped with UPlan(F), 100x/1.30 objective lens (Olympus) and a cooled black/white CCD camera (ORCA-R2, Hamamatsu) under the control of the microscope software CellSens Dimension (Olympus), was used to obtain microscopy pictures. The following fluorescence filters were used: FITC-2024B-000, Txred-4040C-000n and Sp. Aqua HC (Sembrock).
Data analysis	Sanger sequencing data was analyzed using ApE (v2.0.55). For evaluation of the TaqMan SNP genotyping assays, the LightCycler® 480 1.5 Software was used. Black and white microscopy pictures were pseudo-coloured using the Adobe Photoshop 2020 software. Graphs were made using R Studio (Version 1.1.423), Microsoft Excel 2016 and CorelDRAW 2020 (Version 22.1.1.523).

For manuscripts utilizing custom algorithms or software that are central to the research but not yet described in published literature, software must be made available to editors and reviewers. We strongly encourage code deposition in a community repository (e.g. GitHub). See the Nature Portfolio guidelines for submitting code & software for further information.

Data

Policy information about availability of data

All manuscripts must include a data availability statement. This statement should provide the following information, where applicable:

- Accession codes, unique identifiers, or web links for publicly available datasets
- A description of any restrictions on data availability
- For clinical datasets or third party data, please ensure that the statement adheres to our policy

The authors declare that the data supporting the findings are available within the manuscript or Supplementary information. Raw data for Figure 2b, Figure 3a,b and Extended Data Figure 3 are provided as Source Data files.

Field-specific reporting

Please select the one below that is the best fit for your research. If you are not sure, read the appropriate sections before making your selection.

☒ Life sciences ☐ Behavioural & social sciences ☐ Ecological, evolutionary & environmental sciences

For a reference copy of the document with all sections, see nature.com/documents/nr-reporting-summary-flat.pdf

Life sciences study design

All studies must disclose on these points even when the disclosure is negative.

Sample size	No sample-size calculation was performed. To determine plants harboring the inversion, rather large sample sizes were chosen due to the expected low inversion frequency (between 0.5 and 2%; see Schmidt, C., Pacher, M. & Puchta, H. Efficient induction of heritable inversions in plant genomes using the CRISPR/Cas system. Plant J 98, 577–589; 10.1111/tpj.14322 (2019)) and to randomize bias from integration of the Cas9 nuclease. We decided to screen 1600 plants to be able to detect inversions occuring with frequencies of about 0.1%.
Data exclusions	No data were excluded.
Replication	True biological replicates (i.e., independent plants) were used as replicates for statistical analyses. The number of replicates is stated in the Figure legends.
Randomization	After transformation with the T-DNA construct, T1 seeds were selected on 10 selection medium plates and transgenic lines were randomly picked from all 10 plates for propagation. T2 analysis was performed with 40 plants per independent transgenic T2 line which were numbered from 1 to 40 randomly. Phenotypical and fertility analyses were performed by randomly numbering the plant lines and assigning the genotype after analysis. SNP analysis was performed with 400 F2 plants that were randomly picked by randomly numbering plants from 1 to 400.
Blinding	Not required, as samples were processed identically through standard procedures that should not bias the outcome. Phenotypical and fertility analyses were performed by randomly numbering the plant lines and assigning the genotype after analysis.

Reporting for specific materials, systems and methods

We require information from authors about some types of materials, experimental systems and methods used in many studies. Here, indicate whether each material, system or method listed is relevant to your study. If you are not sure if a list item applies to your research, read the appropriate section before selecting a response.

Materials & experimental systems

n/a	Involved in the study
☒	☐ Antibodies
☒	☐ Eukaryotic cell lines
☒	☐ Palaeontology and archaeology
☒	☐ Animals and other organisms
☒	☐ Human research participants
☒	☐ Clinical data
☒	☐ Dual use research of concern

Methods

n/a	Involved in the study
☒	☐ ChIP-seq
☒	☐ Flow cytometry
☒	☐ MRI-based neuroimaging